AD-A114 660 SOUTHERN UNIV BATON ROUGE LA DEPT OF MECHANICAL ENGI--ETC F/G 11/6

AN INVESTIGATION OF MECHANISMS EFFECTING ENVIRONMENTAL STRESS C--ETC(U)

JUL 81 N00019-80-C-0421

UNCLASSIFIED NL

END

DATE FILMED

6-82

DTIC

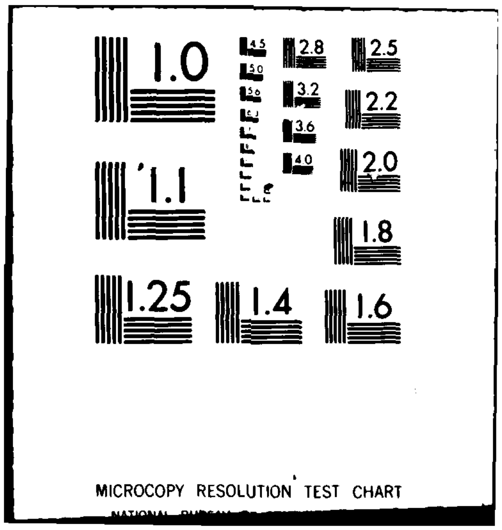
1.0
1.1
1.25
1.4
1.6
1.8
2.0
2.2
2.5
2.8
3.2
3.6
4.0
4.5
5.0
5.6
MICROCOPY RESOLUTION TEST CHART

(1)

"AN INVESTIGATION OF MECHANISMS EFFECTING ENVIRONMENTAL STRESS CRACKING IN TITANIUM ALLOY"

July 6, 1981

Work Performed Under the Direction of
Ira J. Graham
(Director)

Mechanical Engineering Department
Southern University
Baton Rouge, Louisiana 70813

Contract No. N00019-80-C-0421
Naval Air Systems Command
Department of the Navy
Washington, D.C. 20301

"AN INVESTIGATION OF MECHANISMS EFFECTING ENVIRONMENTAL STRESS CRACKING IN TITANIUM ALLOY"

July 6, 1981

Work Performed Under the Direction of
Ira J. Graham
(Director)

Mechanical Engineering Department
Southern University
Baton Rouge, Louisiana 70813

Contract No. N00019-80-C-0421
Naval Air Systems Command
Department of the Navy
Washington, D.C. 20301

Acknowledgements

The investigation period involved the efforts of six upper level Mechanical Engineering students, one junior level Accounting student, the faculty alternate and director. The writer wishes to express appreciation and thanks for the interest and effort given by Corlette Williams, Lisha Washington, Zahra Khossropoor, Arleen Johnson, Ramona Smith, Ralph Wilson and Wardell Bowie. Also thanks goes to Dr. John Tabony for his valuable assistant as the faculty alternate on the project.

Table of Contents

"An Investigation of Mechanisms Effecting Environmental Stress Cracking in Titanium Alloy"

Abstract

A~~n~~ heat treated version of titanium alloy (Ti6Al4V) has been under an environmental stress cracking investigation. The acoustic emission (AE) techniques were used to monitor crack growth in a 1 inch thick WOL bolt loaded compact tension test specimen under a linear compliance load to provide plane strain fracture over the environment test duration. An acoustic emission transducer (S-140B) was used to detect the crack movement in the test specimen while it was submerged in a closed loop metharol environment. The acoustic signals were received at a gain of 85 dB in a high bandpass filter range of 100-300 KHz and displayed in the totalizer window as digital output data, (BCD). The signals were then passed into the D/A converter and recorded as analog data on the x-y plotter.

Two significant results in this investigation were revealed by the AE technique, (1) heat treating just below the beta transformation temperature and annealing for a select time improved the fracture toughness in the alloy, and (2) in a plane strain load mode at a constant crack-opened-displacement (COD), the titanium alloy was crack sensitive in a pure methanol environment and not crack sensitive in the laboratory atmosphere environment. The acoustic emission rate, hence crack growth

rate, appears to be a function of the methanol concentration, thus related to a diffusion mechanism.

Introduction

Titanium alloy (Ti6Al4V) has been located in a closed-loop environment chamber and subjected to a pure grade (99.95%) methyl alcohol (methanol-CH_3OH) at a constant temperature, 78°F (25.6°C) and pressure, 14.7 psi (76.0 cm HG). Since alcohols and acetones have been widely used as degreasing and cleaning agents on many mechanical and hydraulic parts, it was thought that these solutions in the higher concentration may be factors that contribute in crack propogation in the solid materials. Titanium alloy is used as a material for the mechanical and hydraulic parts of the aircraft and much of the degreasing and cleaning of the parts have been done with alcohols and acetones. This research effort on crack propogation in titanium alloy in a methanol environment was started around this analysis. The application of the acoustic emission techniques was to make it possible to detect the crack propogation that were neither audible or visible without amplification or optics.

A bolt-load type wedge-opened-load (WOL) one inch thick compact tension test specimen was drawn to scale, using the specification shown in ASTM-E399-75 standards, Figure 1. Ten of these test specimens were machined in the Mechanical Engineering Department Laboratory; however, only five were used in the investigation

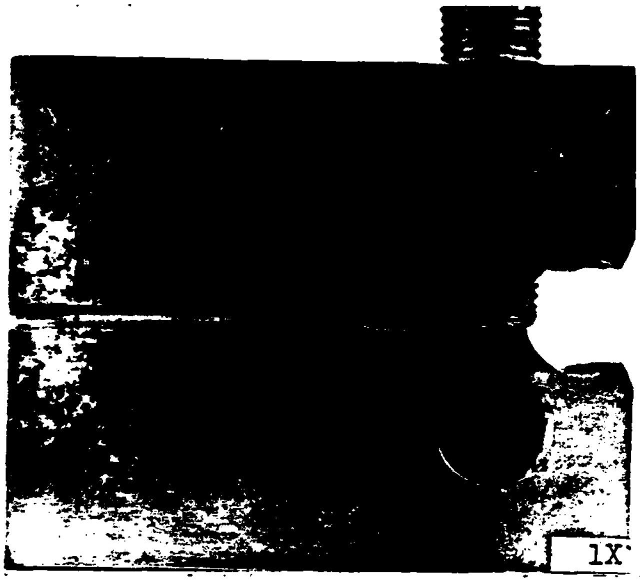

Figure 1. The bolt load IT WOL compact tension test specimen used in this investigation.

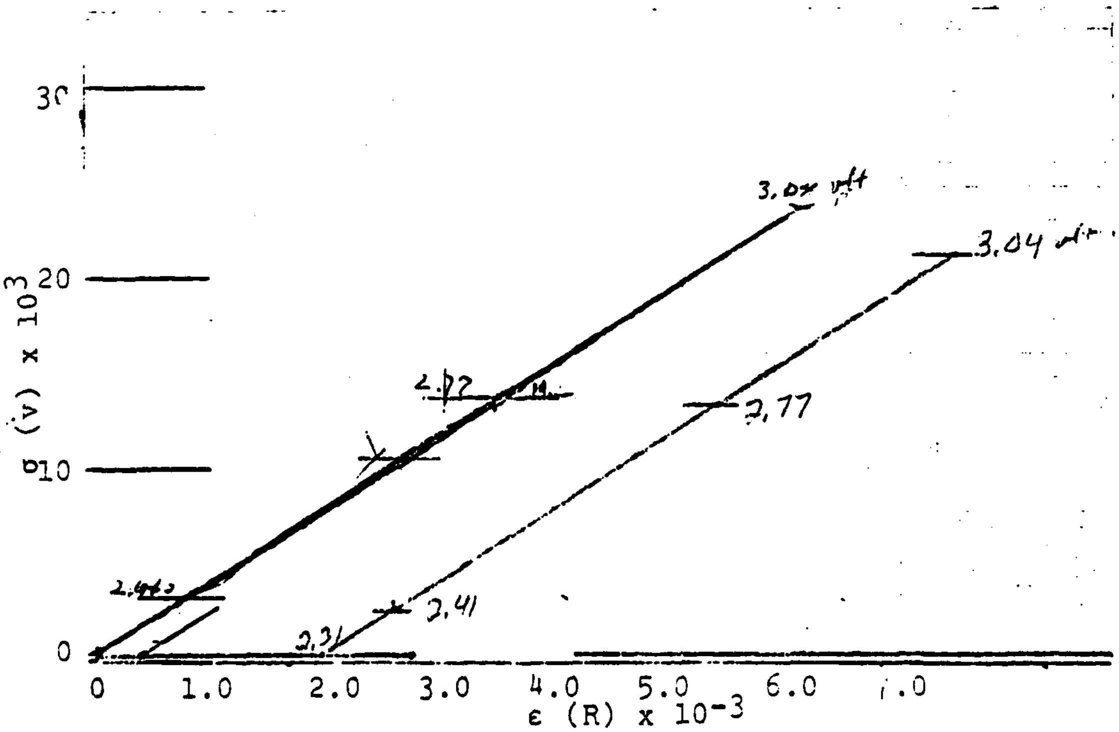

Figure 4. The stress/strain curve plot for the fatigue load in precracking WOL test specimen A-3 and is typical of that for the other test specimens used in this investigation.

for this period. The test specimens were then subjected to a heat treatment process which was designed to increase the fracture toughness of the titanium alloy. The specimens were held as a batch in an electric arc furnace free of CO, CO_2, H_2O and NH_4 just below beta transformation (1630°F (887°C)) for one hour then rapidly water quenched to room temperature. The batch was then returned to the furnace under the same atmosphere controls and annealed at 1050°F (568°C) for 6 hours then allowed to air cool in the laboratory to room temperature.

This heat treat process produced a thin film (.003 in.) of titanium oxide over the surface of the specimens. The thin film was removed by using the wet belt grinder and 50 grit silicon carbide abrasive. This operation required approximately forty minutes per test specimen. All test specimens were finished to the drawing specifications, Figure 16.

Experimental Procedure

The one inch thick bolt load type wedge-opened-load (WOL) compact tension test specimen shown in Figure 1 was found suitable to plane strain fracture toughness and a constant stress intensity factor K_I over approximately 80% of the depth (W) of the specimen. This type test specimen also was capable of maintaining the linear compliance load at a constant crack-opened-displacement (COD) in the closed-loop methanol environment test chamber with the acoustic emission

transducer attached securely for monitoring the crack over the test period. Five test specimens were heat treated at 1630°F (890°C) for 1 hour and water quenched and annealed at 1050°F (568°C) for 6 hours, then cleaned for testing. The following equation, $\Delta P = \Delta K(B_n\sqrt{w})/f(a/w)$[1], was used to determine the linear compliance load for producing the fatigue precrack in each of the test specimen used in the investigation and the w = the depth of the test specimen, a = crack length, f = a constant, B_n = specimen thickness and ΔK = stress intensity change determined by the 5% secant offset method.[3] The test specimen was loaded in the 22 kip servo-electronic dynamic testing machine and the MTS clip gage was fitted between the knife edges on the specimen to act as the strain control device during the fatigue precrack period. The multimeter was used to determine the desired voltage which was converted to load (ΔP) in pounds for the fatigue precrack. Figure 4 shows the linear compliance load plot for the fatigue precrack in test specimen A-3. This is typical for the other test specimens except that the loads varied, Table 1, 2, and 3. A set load of 200 lbs. (888 N) was applied on all test specimns to maintain a tension to tension fatigue precrack mode. Test specimen A-2 was accidentally failed when the load limit switch was set beyond the calculated fatigue precrack amplitude, Figure 15(a).

The precracked test specimens were given a bolt load linear compliance by use of the multimeter, MTS clip gage and the bolt

5/8-18NF 2B. The acoustic emission transducer was located on the face surface side with a viscuous resin and tape after which the specimens were observed in the laboratory atmosphere condition, 78°F (25.6°C) 48% humidity, for periods between 36 hours and 48 hours to see if the precracks grew. Following this period the test specimen with the attached transducer was placed in the closed-loop environment test chamber. The chamber was purged with a dry grade of nitrogen gas at 3 cubic feet per hour for 30 minutes while the high purity methanol (99.5%) was funneled into the chamber from the bottom to the upper level of the machined groove on the test specimen.

The traveling microscope (32X) was focused to the precrack tip and used to follow the crack growth at the surface. The acoustic emission data were recorded on the x-y plotter. After the crack arrested, the test specimen was removed from the methanol environment, wiped and allowed to remain in the laboratory atmosphere up to 12 hours for additional crack growth observation monitored by the acoustic emission system. The crack-opened-displacement was checked with the MTS clip gage and multimeter, then the test specimen was completely fractured by continuing the bolt loading, Figure 2(a)(b)(c).

Macrophotographs (2.5X) were made of the cracked surfaces, Figures 3(a)(b)(c). Sections were cut from the specimens, mounted and prepared as micro-structures. Micrographs were made of the etched specimens as seen in Figures 11, 12, 13, and 14.

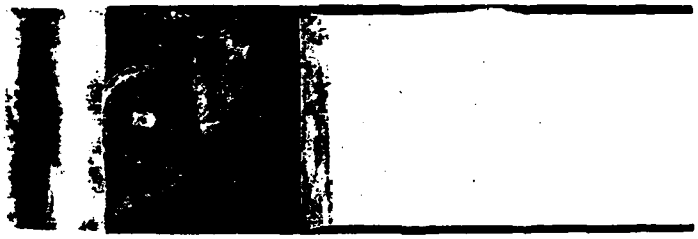

(a)

1.4X

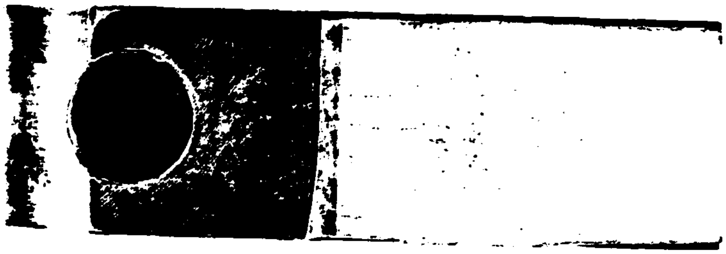

(b)

1.4X

(c)

1.4X

Figure 2 a,b,c. Macrographs of the test specimens that have been under a linear compliance load during a test period. The methanol environment stress cracked surface is readily identified.

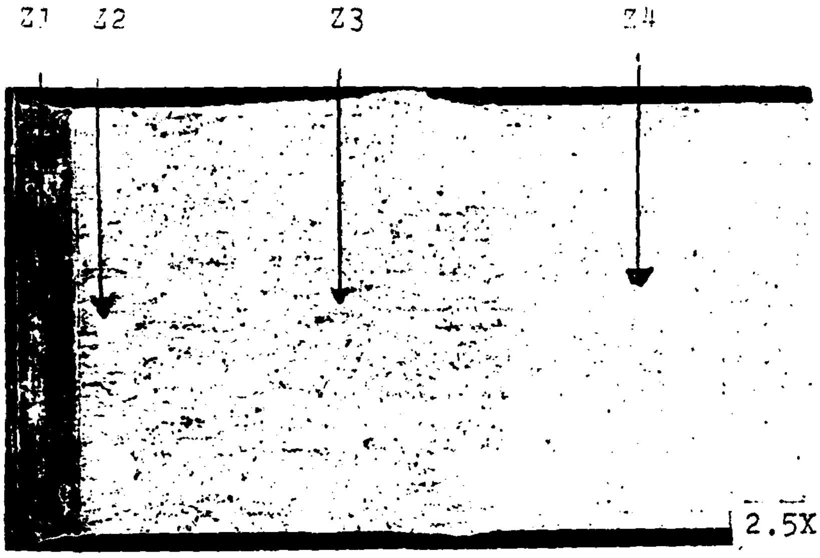

(a)

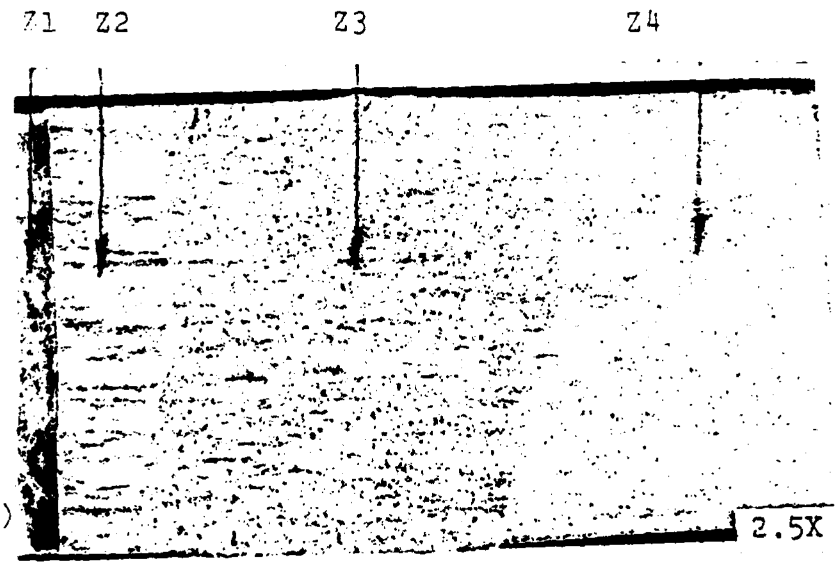

(b)

Figure 3 a,b. The enlarged macrographs of two test specimens seen in Figure 2, show four different fractures, Z1-machined V-notch, Z2-fatigue precrack, Z3-methanol environment stress cracking and Z4-tensile fracture.

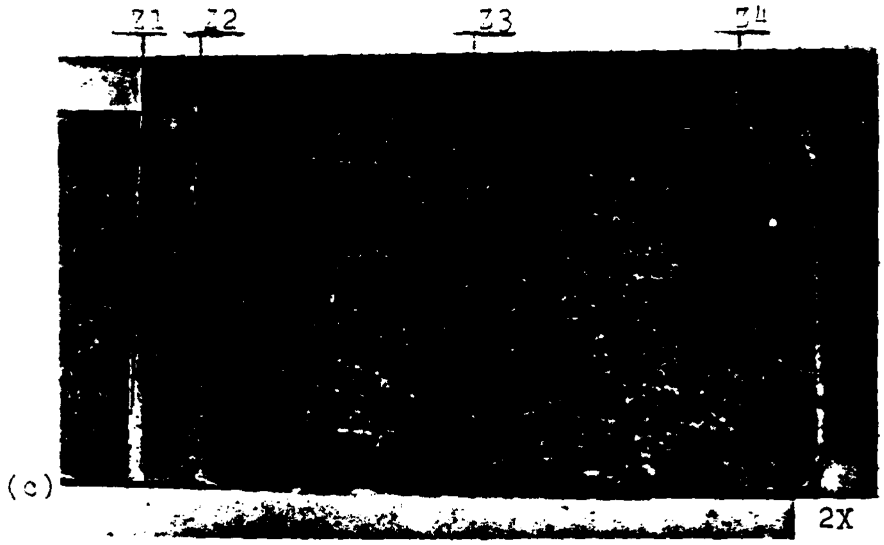

Figure 3 c. The enlarged macrograph of the test specimen seen in Figure 2, shows four different fractures, Z1-machined V-notch, Z2-fatigue precrack, Z3-methanol environment stress cracking and Z4-tensile fracture.

Kroll reagent was used as the etchant to bring out the grain structure of the polished titanium alloy (Ti6Al4V). A few dark spots less than 0.1 mm were observed in the microstructure at 100X. These appeared to be transverse to the rolling direction of the as received mill annealed alloy.

The microcracks produced under the influence of the methanol environment stress cracking condition were examined for transgranular and intergranular effects in the grain structure. The grain structure was examined for the type structure and the solution heat treat and aging effect.

Discussion of Results

The information available indicated that the titanium alloy (Ti6Al4V) under investigation is the alpha-beta grade and that the strength properties can be improved through proper solution heat treatment and annealing[4]. The investigation in this research effort was to involve a solution heat treated version of the titanium alloy. Five test specimens were batch solution heat treated at 350°F (176°C) per hour in a vertical gantry electric arc furnace and a 1630°F (890°C) for one hour and rapidly water quenched in less than 5 seconds. Annealing occurred at 1050°F (568°C) over a 6 hour period and air cooling in the laboratory atmosphere, 78°F (25.6°C) about 58% humidity. Three advantages were expected; (1) less beta transformed to cause martensite structure on quenching, (2) less distortion and titanium oxide occurs at the surface on quenching,

and (3) improved yield strength, hence fracture toughness is increased.

High purity grade methanol (CH_3OH) 99.5% has positive effect on crack propogation when the concentration is sufficient to flow into the crack zone. The acoustic signals occur in burst and continuous form with long arrest periods between crack movement, Figure 5. Crack propogation was not detected in the test specimens under the compliance load by the acoustic emission system at an 85 dB gain in the 100-300 KHz range and was not observed on the surface through the traveling microscope (32X) while the test specimens were in the laboratory atmosphere, 78°F (25.6°C) and 42% humidity. The same test specimens, when exposed in the methanol environment began to emit acoustic signals in less than 20 minutes.

The data given in Tables 1, 2 and 3 represent the findings from three test specimens out of five that were designed and made for the investigation. Test specimens A-2 and A-5 were lost by human errors. The calculations are more complete on test specimen A-4.

Figure 5 shows the acoustic emission amplitude and crack arrest period. The acoustic signals indicate that the crack starts as a high amplitude burst followed by the arrest periods that range from 2 to 60 minutes. The long arrest periods between burst type acoustic signals is probably related to the time required for the methanol to reach a sufficient concentration

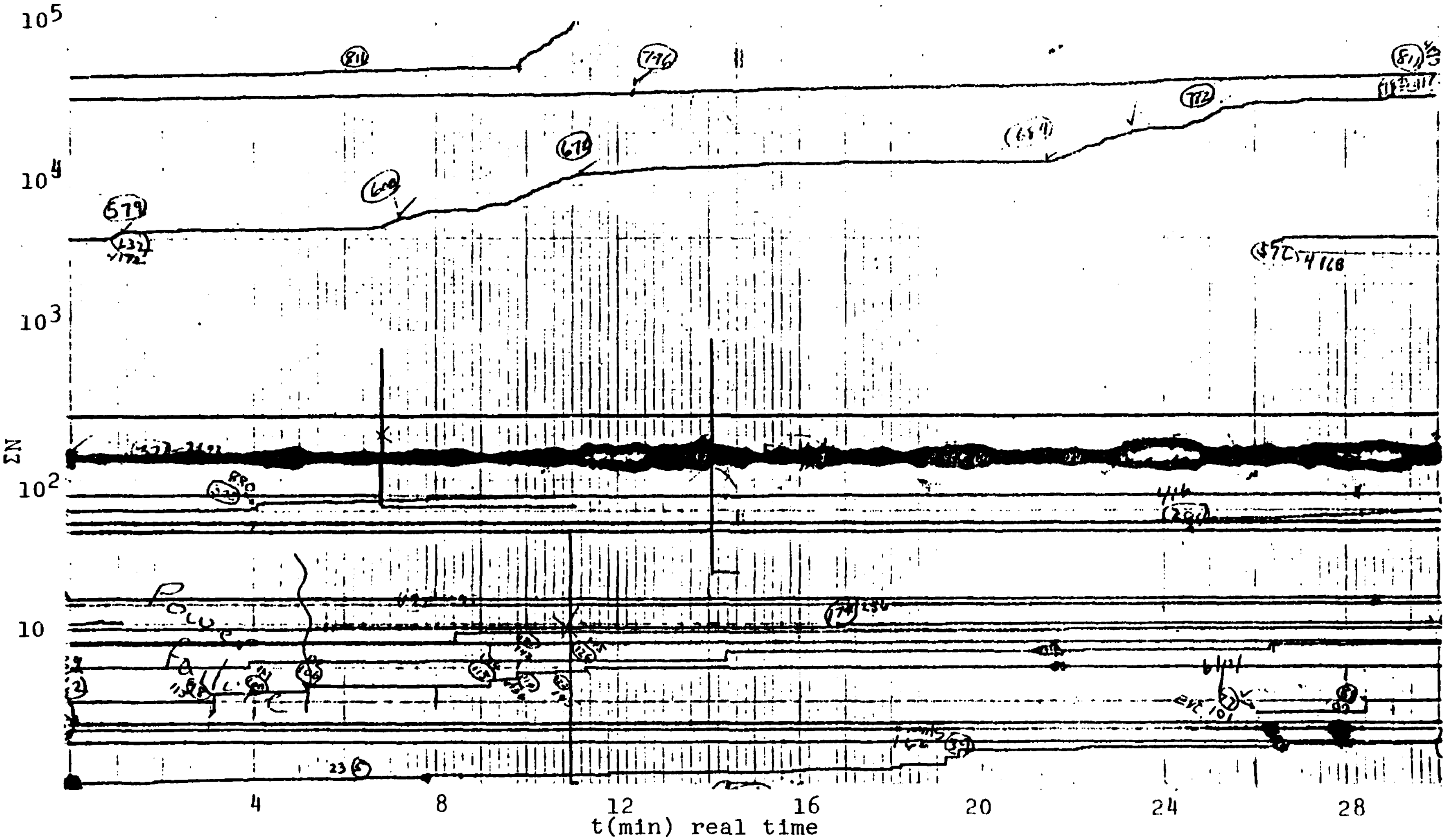

Figure 5. The acoustic emission signals taken from test specimen A-4 while under a compliance load (ΔP) of 2000 lbs. and in the closed-loop methanol (CH_3OH) environment.

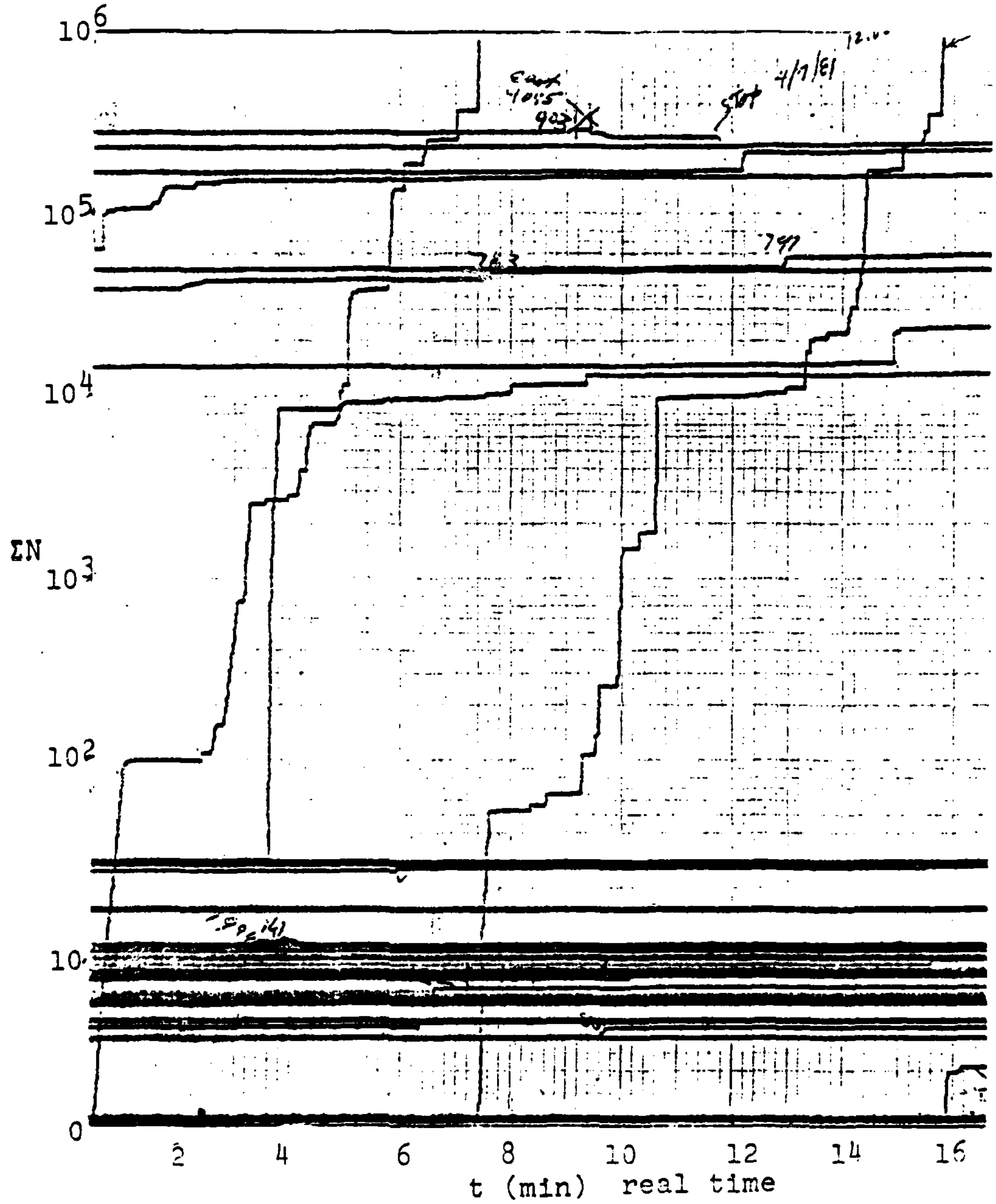

Figure 6. The heavy lines represent the crack arrest periods, while the high amplitude peaks indicate burst type crack movements.

level in the microcracks area. The continuous emission extends over longer growth periods and in one ocassion the crack was observed moving along the surface of the test specimen. Figure 6 shows the continuous emission and intermittant high amplitude. Fourteen hours after the last high amplitude plot shown in Figure 6, the acoustic signals were no longer being emitted. The crack length was measured and a critical stress intensity (K_{1c}) was found to be 74.79 Ksi$\sqrt{in}$ (82.8 MPa$\sqrt{m}$). The relationship of the stress intensity to the crack length was determined by the following equation, $K_1 = P_c/B_n\sqrt{W}[29.6(a/w)^{1/2} - 185.5(a/w)^{3/2} + 655.7(a/w)^{5/2} - 1017.0(a/w)^{7/2} + 638.9(a/w)^{9/2}]$(3). Figure 8 shows the stress intensity at the calculated compliance loads. The linear compliance load was decreased on each test specimen for the environment stress cracking so that a minimum plastic region was at the precrack tip. This had a slowing effect on the crack growth rate and reduced the critical stress intensity factor (K_c) over the range of the crack, Tables 1, 2 and 3.

The data taken from test specimen A-4 on the crack growth rate ($\Delta a/\Delta t$) to the stress intensity (K_c) over the crack growth range indicate a slow moving crack with a decreasing relationship to the stress intensity during the methanol environment attack, Figure 9. Over the same crack growth period, the acoustic signal rate (dN/dt) showed a randomly scattered relationship to the stress intensity. The scatter approaches a constant relationship, Figure 10. This does not agree with the work of other

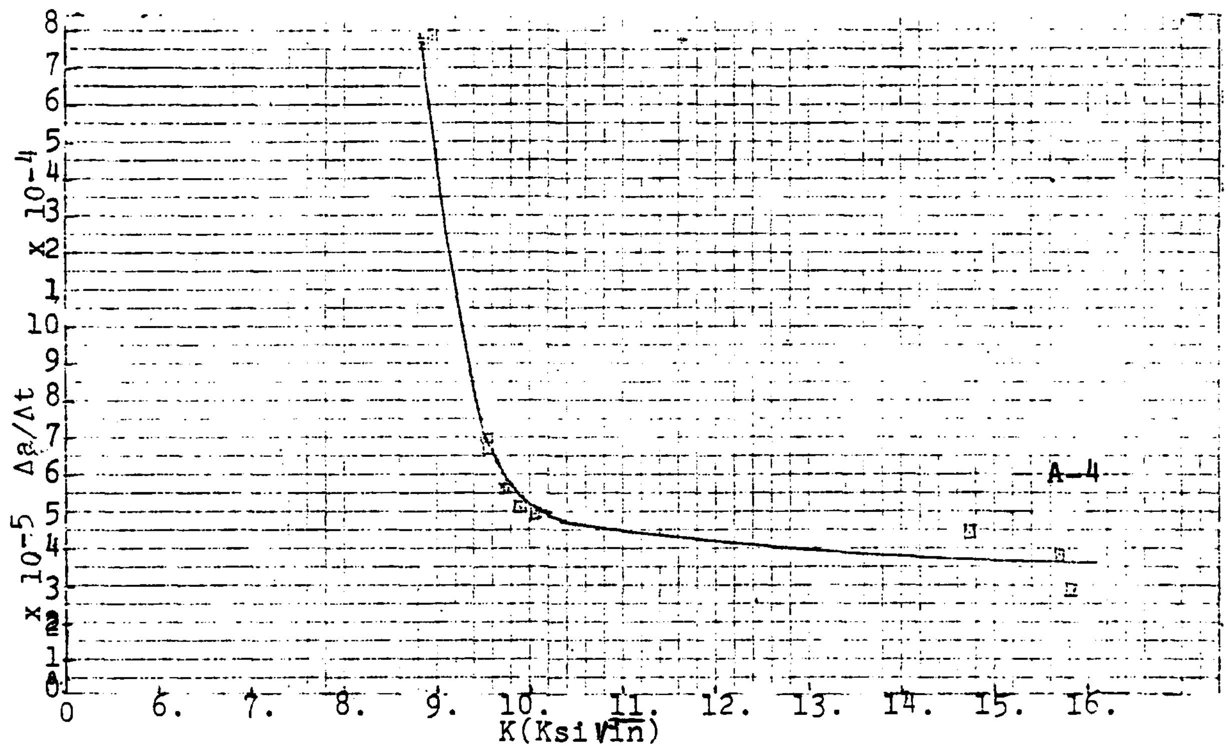

Figure 9. The rate of change in crack length was found to be decreasing with the stress intensity (K_c) in the test specimens.

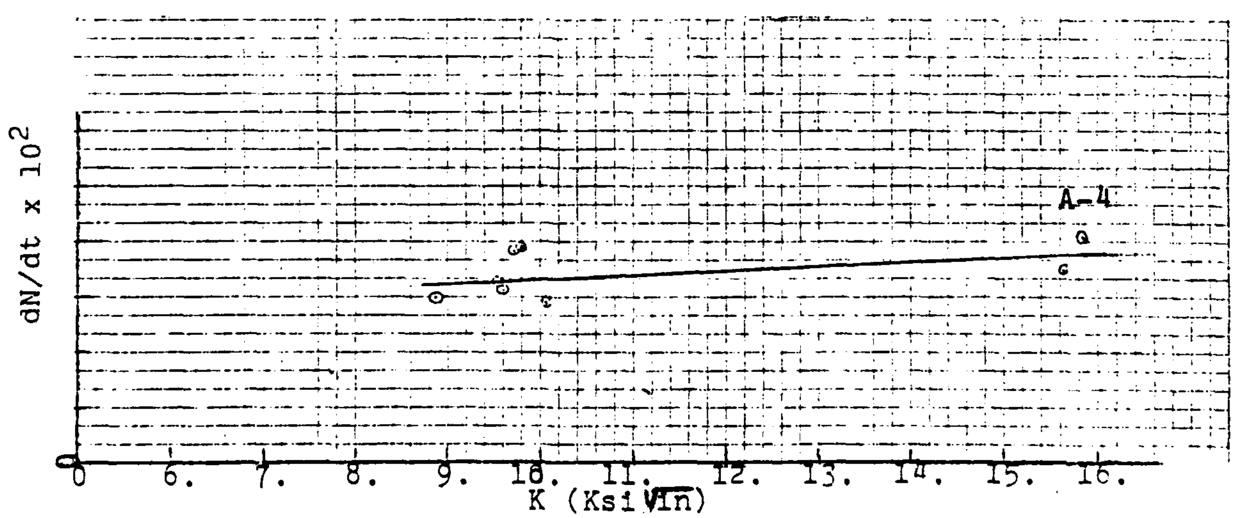

Figure 10. The rate of change of the acoustic emission with the stress intensity (K_c) over the crack range.

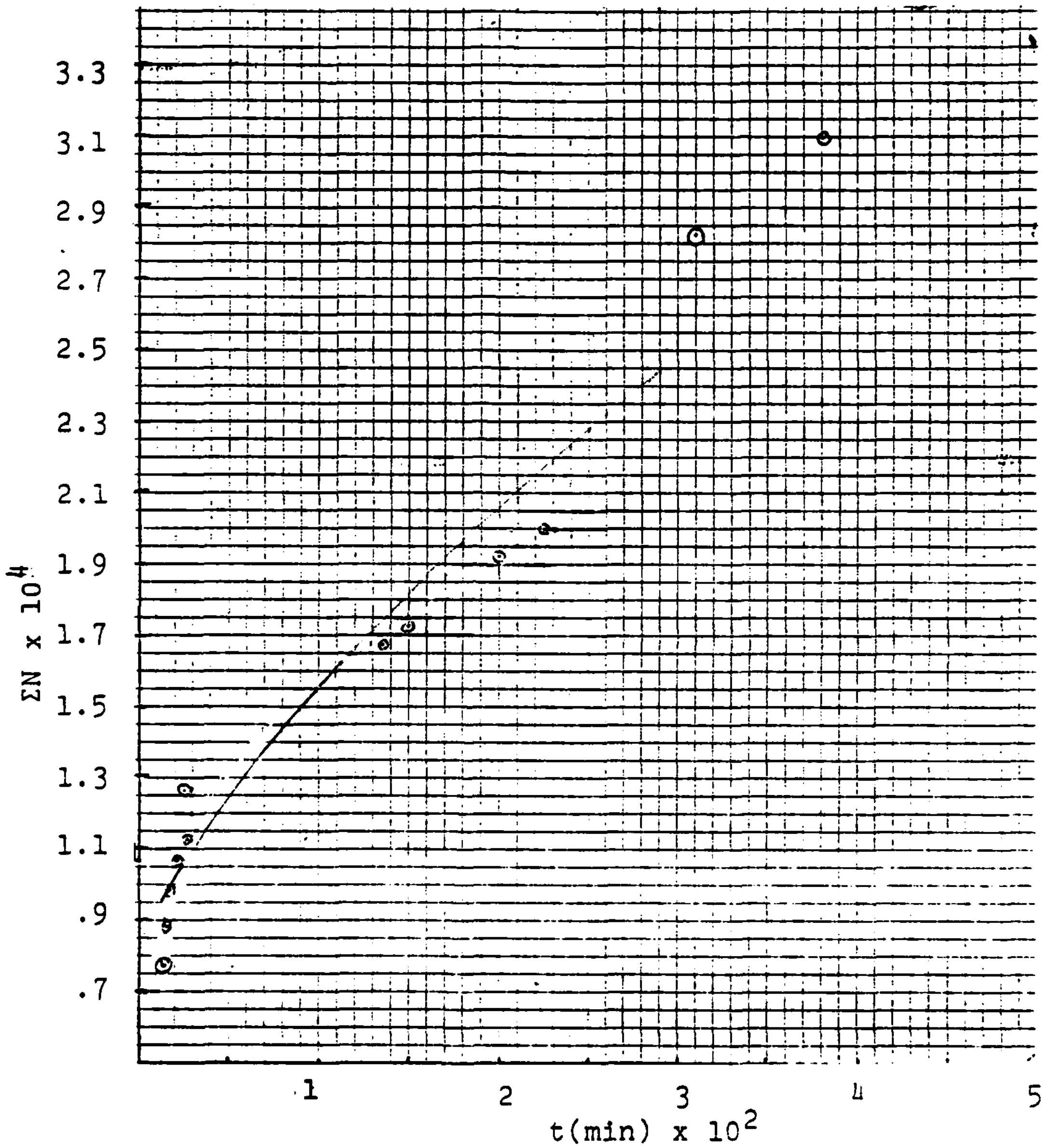

Figure 7. The acoustic emission output with respect to time during the crack growth.

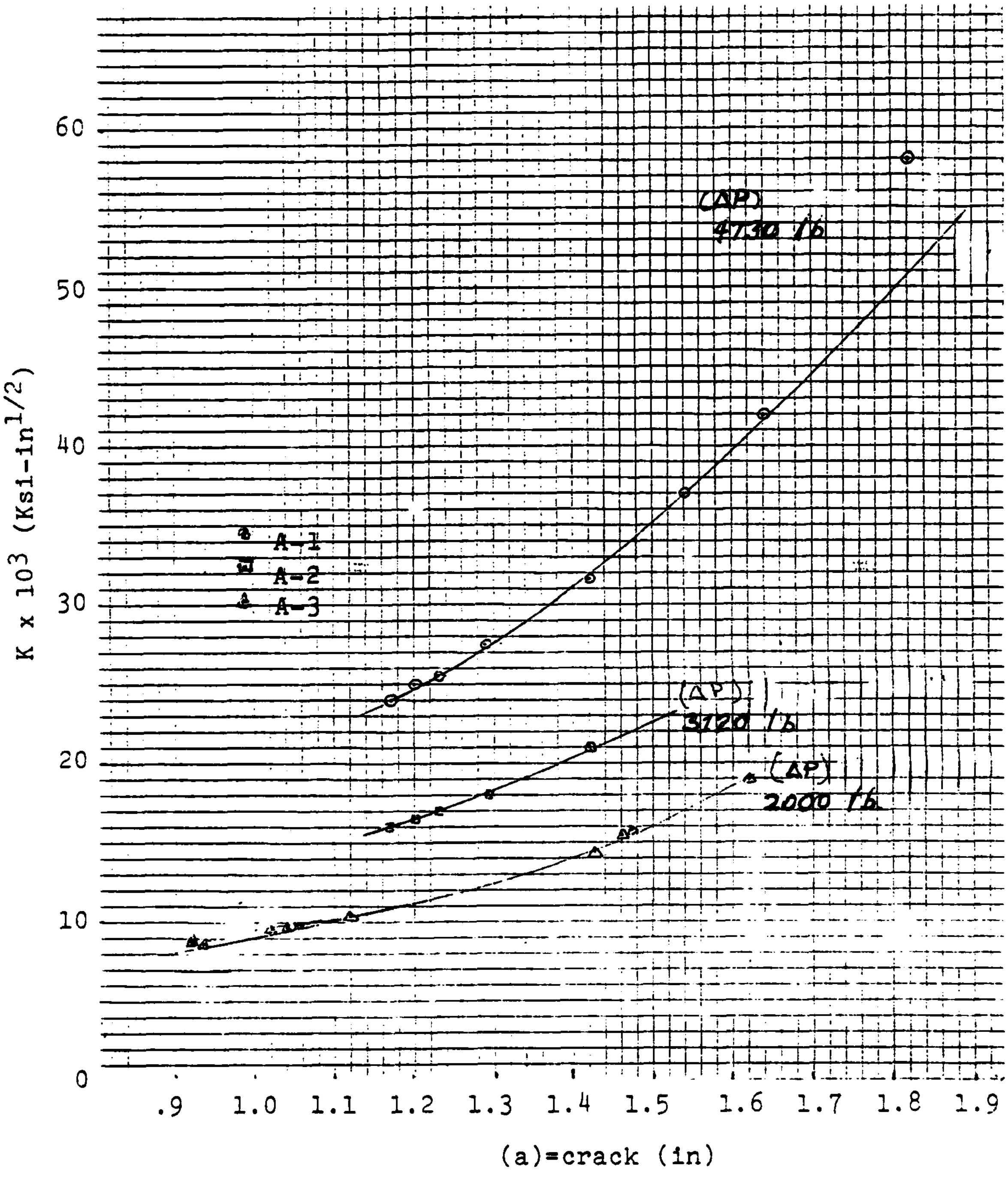

Figure 8. The relationship of the stress intensity (K_{1c}) to the crack growth (a) under the influence of the methanol environment.

investigators, Dunegan, H and Tetelman, A.[6] Further investigation will be pursued in this area. The summation of acoustic signals (ΣN) are shown to be an increasing function with time (t) of crack growth, Figure 7. Other investigators have shown similiar data.

The microstructure shown in Figure 11 represents the type alpha-beta grains found in the other test specimens. Small areas of the Widmanstätten structure were found in the environment stress crack zone, Figure 13. The methanol environment stress cracking is characterized as pit corrosion type cracks which occur as transgranular and intergranular cracks and is readily distinquishable from fatigue and tensile type surface fracture. The fatigue and tensile fracture show fairly straight edge effect in contrast to the valley and mountain effect. The grain structure is uniform with slightly elongated geometry. Some small inclusions were found in the microstructure transverse to the rolling direction.

Figure 13 shows the pit formation along the surface that has been exposed to the methanol environment. Small intergranular cracks are seen below the surface.

Conclusions

1. Cracks, some which grow at less than 10^{-5} inch per hour, are difficult to detect on the surface of titanium alloy without the aid of magnified optics.

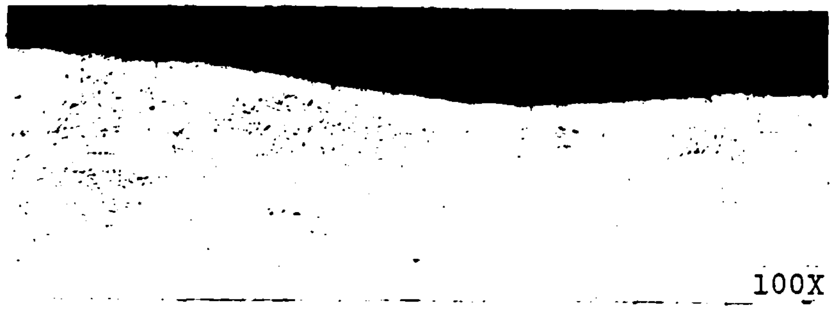

Figure 11. The micrograph shows an acicular type grain structure of uniform size. A regular flat surface along the microstructure indicates a fatigue crack surface followed by a slightly irregular methanol environment stress crack.

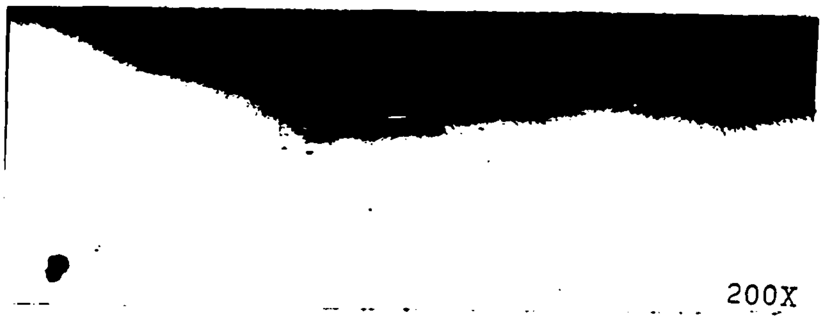

Figure 12. The micrograph shows a uniform a icular grain structure. At the right, a flat regular fatigue surface is followed by the irregular methanol environment stress cracked surface.

Figure 13. The micrograph shows the methanol environment stress cracked surface containing pit holes and the irregular surface. The transgranular cracks are seen below the surface.

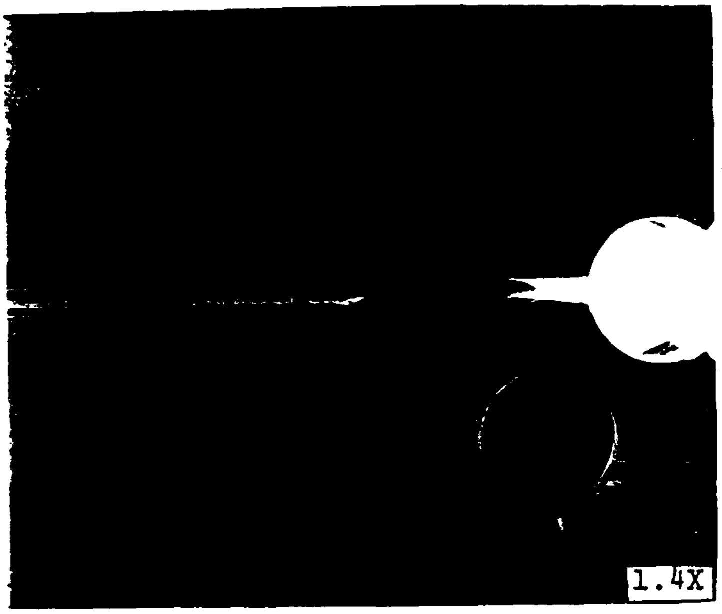

Figure 15a. The macrograph of the 1T WOL compact ension test specimen A-2 with the uncontrolled crack that occurred with an accidental increase in the amplitude of the compliance load.

Figure 15b. Enlarged macrograph of the uncontrolled crack in test specimen A-2.

2. A crack of any size in titanium alloy (Ti6Al4V) under a stress intensity (K_1) of 8.1 Ksi$\sqrt{in}$ (8.86×10^{-3} MPa$\sqrt{m}$) or greater when exposed to a concentrated methanol environment over a 20 minute period will exhibit growth.

3. Methanol environment stress cracking in titanium alloy is slow diffusion type mechanism that produces the pit corrosion effect and is detectable by the acoustic emission technique.

4. The bolt-load type compact tension specimen is an effective vehicle for determining environment stress cracking rate behavior and the critical stress intensity factor (K_{1c}).

5. The acoustic emission approach to studying environment stress cracking may prove to be of great value in determining the mechanism.

6. The continuous acoustic emission with intermittant high amplitude indicate that the fracture is in an unstable. condition and approaching failure.

7. More acoustic emission work with crack growth behavior need be conducted in order to relate the amplitude per unit acoustic signal to a quantative energy value.

8. The microstructure of the solution heat treated and annealed Ti6Al4V exhibited the acicular alpha structure with small areas of the Widmanstätten pattern.

9. The environment stress cracking appeared in the Widmanstätten structure in transgranular type cracks.

References

1. Wright, C. P., "Development of An Acoustic Emission Inspection Technique for Hydraulic Components With Moveable Parts", Instrument Society of America, Pittsburgh, Pa. 1976.

2. 1978 Annual Book of ASTM Standards, Part 10, ASTM Philadelphia, Pa, E 399-74, 1978.

3. Fracture and Fatigue Control in Structure, Rolfe, S. T. and Barsom, J. M., Prentice-Hall, N.J. 1977.

4. Source Book on Heat Treating, Vol. 1 "Materials and Process", ASM Metals Park, Ohio, pp 254-367, 1975.

5. American Society for Metals Handbook 8th Edition, Vol. 7, Microstructures of Industrial Alloys, pp 322-334, 1973.

6. Dunegan, H. L. and Tetelman, A. S., "Non-Destructive Characterization of Hydrogen-Embrittlement Cracking By Acoustic Emission Techniques", Pergamon Press, Oxford, N.Y. 1970.

7. "Properties of Ti6Al4V", Titanium Metals Corporation of America, Titanium Engineering Bulletin No. 1, 1965.

8. Harris, D. O., "The Effect of Gain and Frequency Bandpass on Acoustic Emission Observed From Growing Fatigue Cracks", Jan. 1974, Dunegan/Endeveco, San Juan Capistrano, Calif.

9. Harris, D. O., "A review of Aerospace Applications of Acoustic Emission", Instrument Society of America, Pittsburgh, Pa. 1976.

10. Kuhn, B. A., "Acoustic Emission Monitoring of Ring-Cracking in Glass and Alumina", Laurence Livermore Laboratory, Livermore, Calif. 1972.

Table 1. Data obtained from test specimen A-4 at a linear compliance load (ΔP) of 2000 lbs. under methanol enviroment stress cracking.

a		K		N X 10^3		t X 10^2		$\frac{\Delta a}{\Delta t}$
in.	mm	ksi$\sqrt{in}$	MPa$\sqrt{m}$	ΣN	dN	$\frac{dn}{dt}$	t	
.922	23.418	0	0	0	0	0	0	0
.927	23.545	8.64	9.56	77	77	6.64	11.6	7.99X10^4
.938	23.825	8.85	9.79	89	12	3	12.0	7.8 X10^4
.938	23.825	8.85	9.79	106	17	1.93	20.8	7.8 X10^4
.938	23.825	8.85	9.79	126	20	3.2	26.9	7.8 X10^4
1.027	26.0858	9.51	10.52	168	42	.34	135.9	7 X 10^5
1.0414	26.451	9.568	10.59	174	6	.36	152.7	6.8X10^5
1.0426	26.482	9.71	10.74	—	—	—	—	6.0X10^5
1.058	26.873	9.803	10.85	194	20	.39	203.9	5.6X10^5
1.128	28.651	10.405	11.52	200	6	.27	225.9	4.99X10^5
1.431	36.347	14.797	16.38	284	84	.99	310.7	4.6X10^5
1.466	37.236	15.633	17.31	309	75	.36	380.1	3.85X10^5
1.475	37.465	15.803	17.49	371	62	.41	532.7	2.79X10^5

Table 2. Data obtained from test specimen A-3 at a linear compliance load (ΔP) of 4730 lbs. under methanol enviroment stress cracking.

a		K		* $\Sigma N \times 10^3$	* $t \times 10^2$
in.	mm	ksi$\sqrt{in}$	MPa$\sqrt{m}$		
1.71	43.434	24.31	26.91		
1.203	30.556	25.07	27.752		
1.234	31.34	25.887	28.656		
1.297	32.943	27.634	30.59		
1.421	36.093	31.818	35.222		
1.546	39.268	37.34	41.339		
1.64	41.656	42.762	47.337		
1.828	46.431	58.726	65.008		

*Data Not Available

K in ksi$\sqrt{in}$ X .001107 = K in MPa$\sqrt{m}$

Table 3. Data obtained from test specimen A-1 at a linear compliance load (ΔP) of 3120 lbs. under methanol enviroment stress cracking.

a		K_I		* ΣN X 10^3	* t X 10^2
in.	mm	ksi$\sqrt{in}$	MPa$\sqrt{m}$	——	——
1.71	43.434	16.032	17.747		
1.203	30.556	16.538	18.307		
1.234	31.34	17.075	18.902		
1.296	32.943	18.228	20.178		
1.42	36.093	21.0	23.247		

*Data Not Available

K in ksi$\sqrt{in}$ X .001107 = k in MPa$\sqrt{m}$

APPENDIX

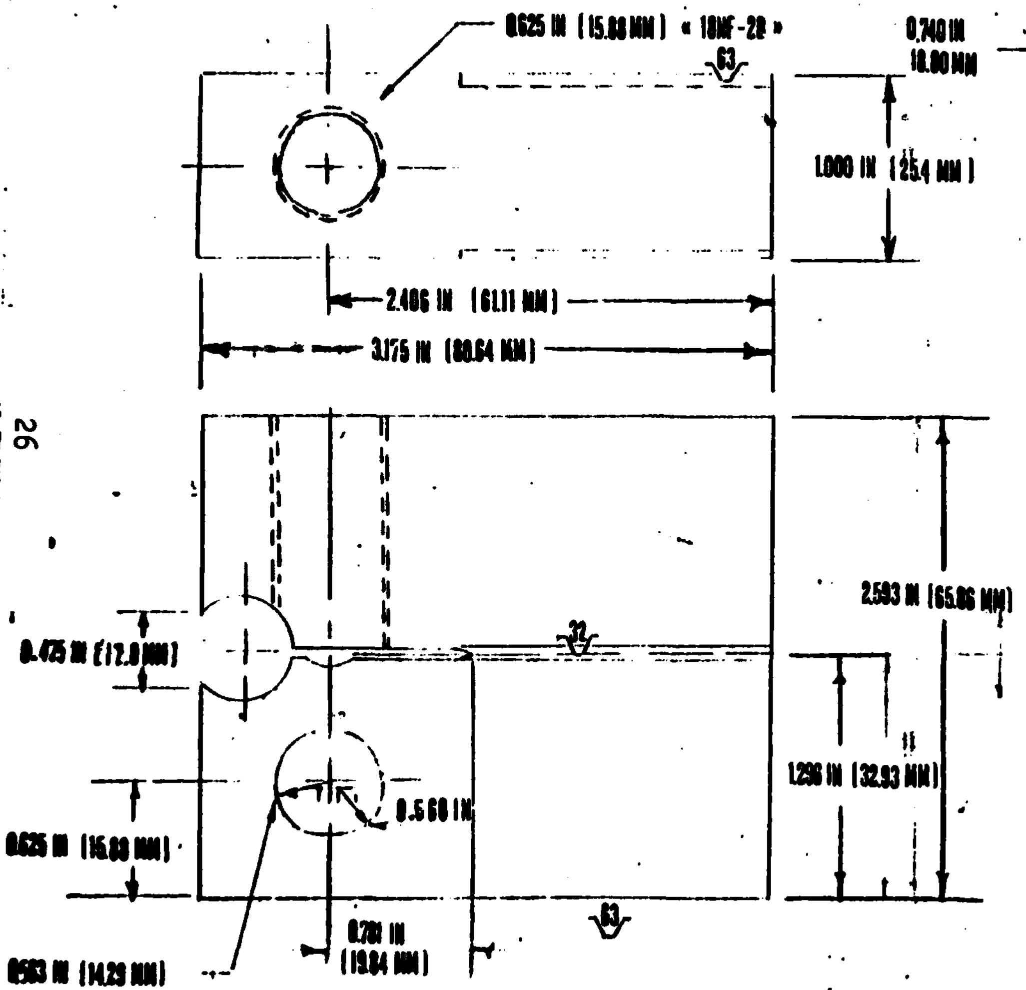

FIG. 1B. WOL (1T) SPECIMEN
(1 INCH THICK)

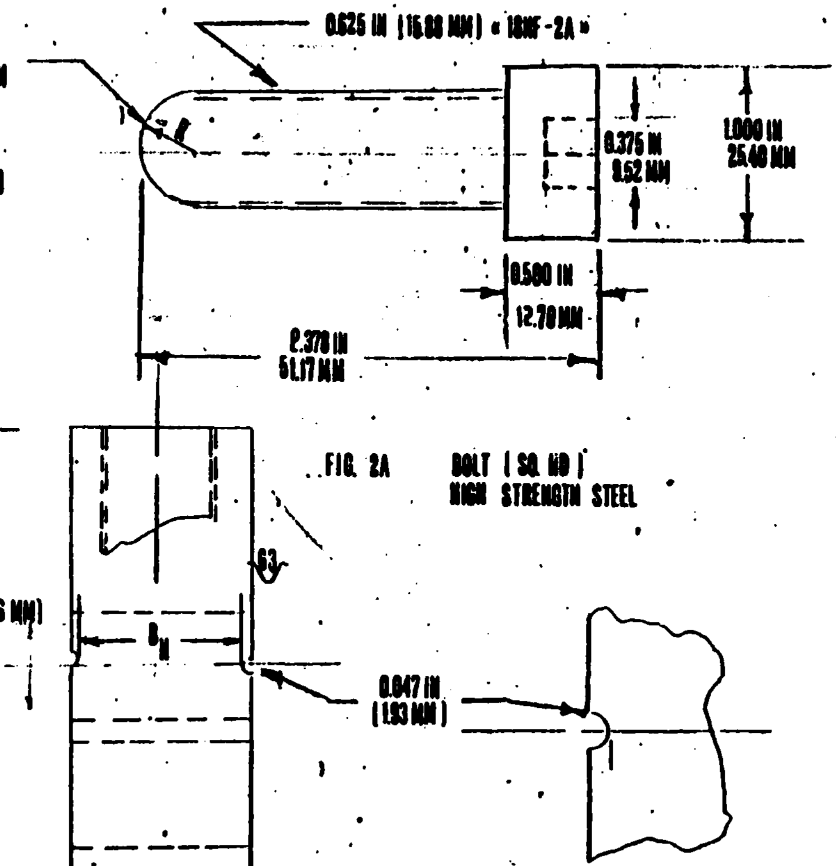

FIG. 2A BOLT (SQ. HD)
HIGH STRENGTH STEEL

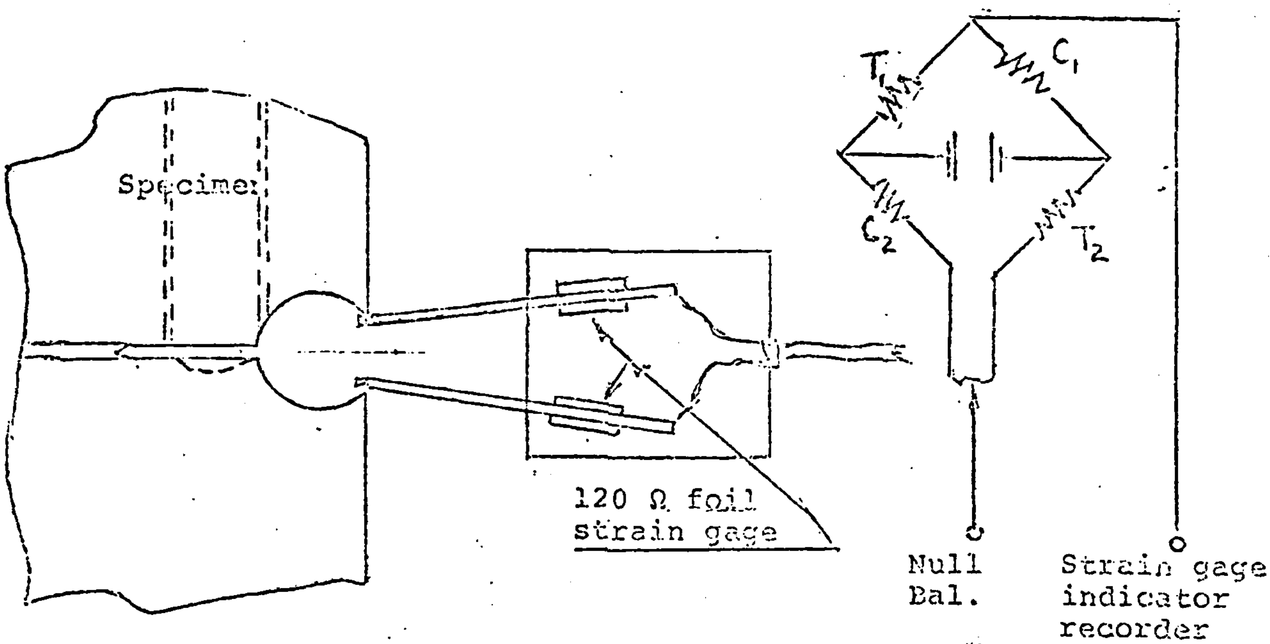

Figure 17. Double cantilever beam strain gage and method of mounting on specimen and measuring displacement; thus load compliance.

The method of employing electric resistance strain gages mounted on a suitably designed flexural element to measure the notch opening under a designed load has been used by other experimenters.

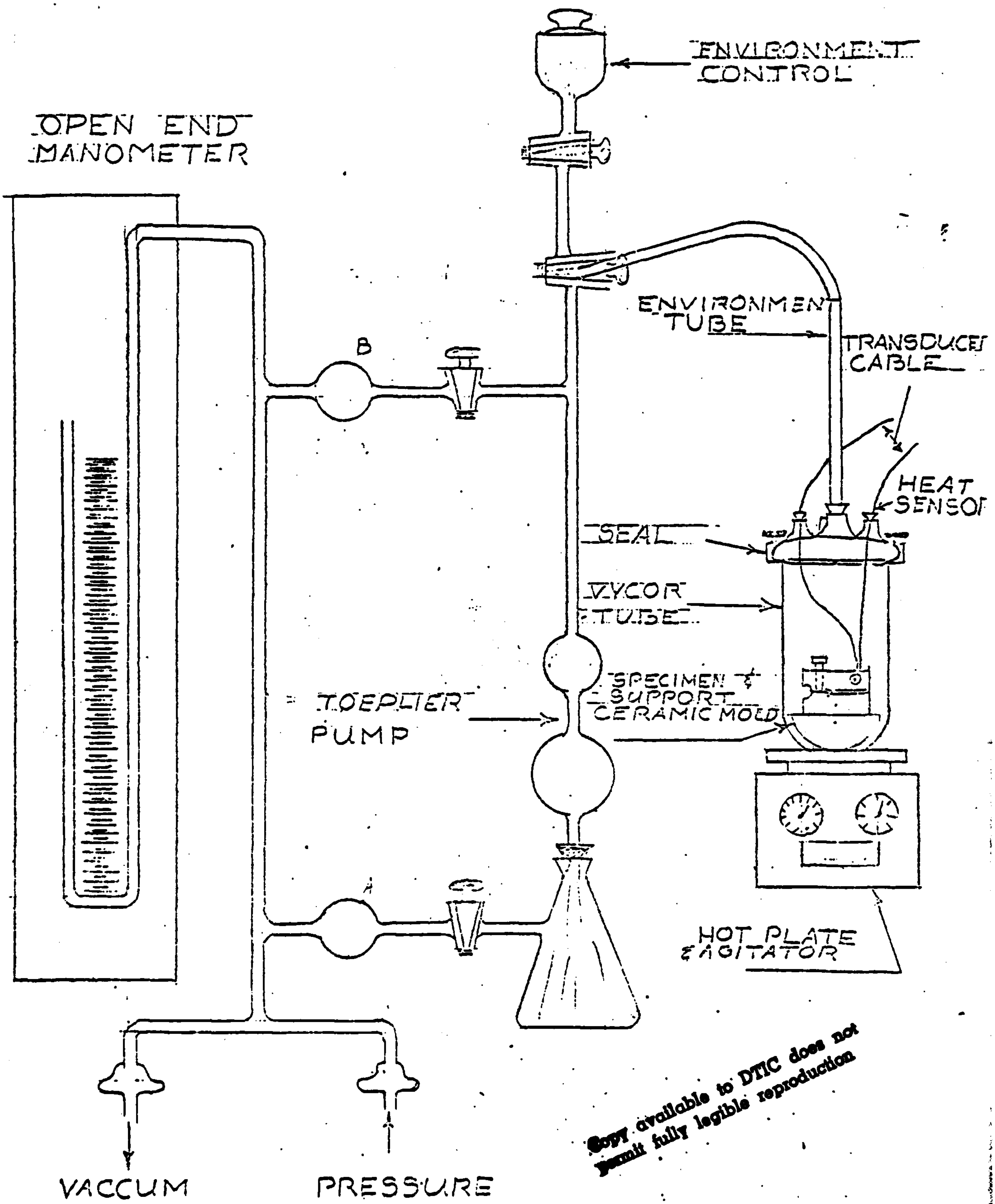

Figure 13.
Environment charging system. Specimen supports on a glazed ceramic mold without Vycortube.

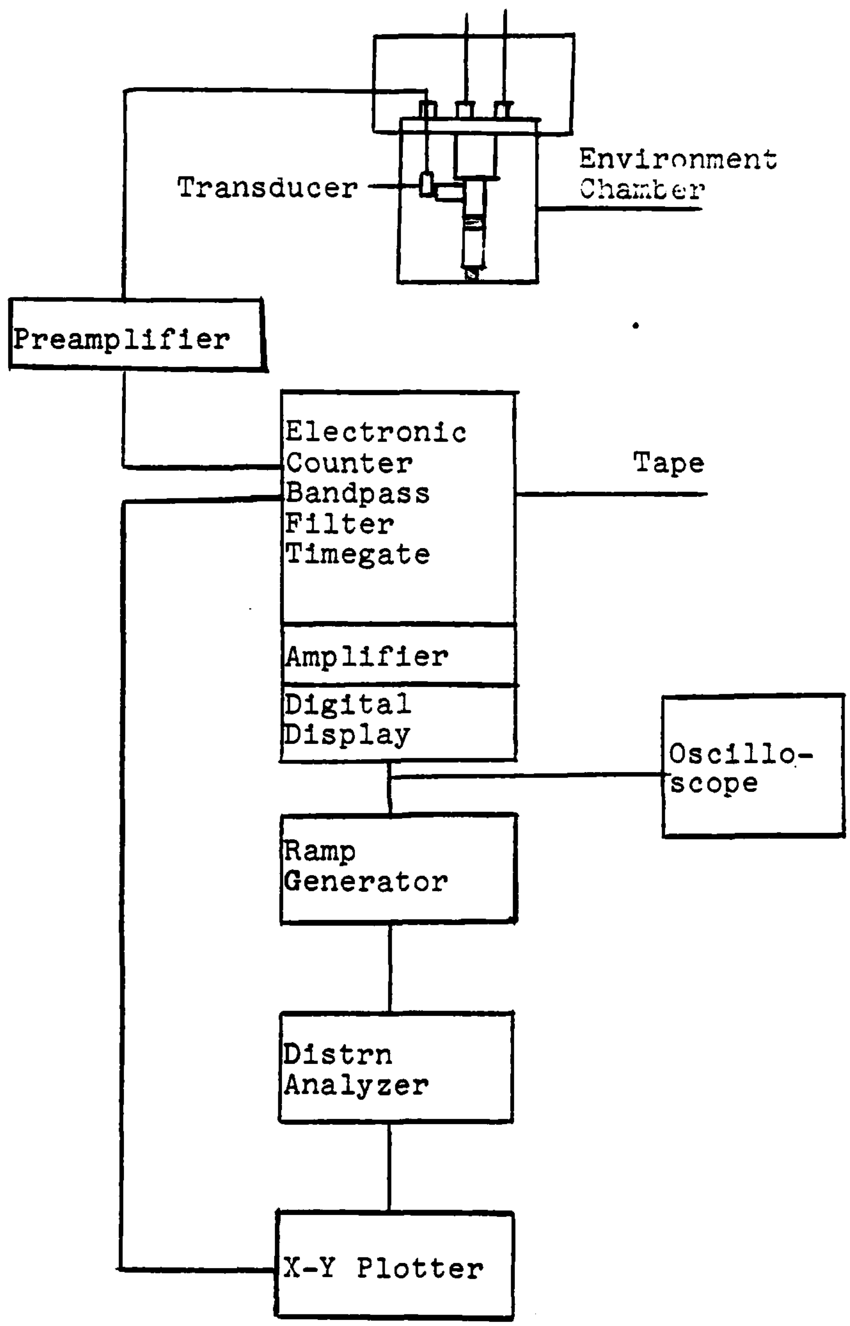

Figure 19. Acoustic emission instrumentation for the environmental chamber.